RSC Advances

PAPER

View Article Online
View Journal | View Issue

Cite this: *RSC Adv.*, 2024, **14**, 433

Interpretation of the adsorption process of toxic Cd^{2+} removal by modified sweet potato residue

Yu Gao, [a] Zhuolin Yi,[a] Jinling Wang,[b] Fan Ding,[c] Yang Fang,[a] Anping Du,[a] Yijia Jiang,[a] Hai Zhao*[a] and Yanling Jin*[a]

Cadmium (Cd) is a common and toxic non-essential heavy metal that must be effectively treated to reduce its threat to the environment and public health. Adsorption with an adsorbent, such as agricultural waste, is widely used to remove heavy metals from wastewater. Sweet potato, the sixth most abundant food crop worldwide, produces a large amount of waste during postharvest processing that could be used as an economic adsorbent. In this study, the feasibility of using sweet potato residue (SPR) as an adsorbent for Cd^{2+} adsorption was assessed. To enhance the removal rate, SPR was modified with NaOH, and the effects of the modification and adsorption conditions on the removal of Cd^{2+} from wastewater were investigated. The results showed that modified sweet potato residue (MSPR) could be adapted to various pH and temperatures of simulated wastewater, implying its potential for multi-faceted application. Under optimized conditions, the removal of Cd^{2+} by MSPR was up to 98.94% with a maximum adsorption capacity of 19.81 mg g^{-1}. Further investigation showed that the MSPR exhibited rich functional groups, a loose surface, and a mesoporous structure, resulting in advantageous characteristics for the adsorption of Cd^{2+}. In addition, the MSPR adsorbed Cd^{2+} by complexation, ion exchange, and precipitation during a monolayer chemisorption adsorption process. This work demonstrates a sustainable and environment friendly strategy for Cd^{2+} removal from wastewater and a simple approach for the preparation of MSPR and also revealed the adsorption mechanism of Cd^{2+} by MSPR, thus providing a suitable adsorbent and strategy for the removal of other heavy metals.

Received 9th October 2023
Accepted 30th November 2023

DOI: 10.1039/d3ra06855b

rsc.li/rsc-advances

1. Introduction

Cadmium (Cd) is a common and toxic non-essential heavy metal, which is mostly found in industrial wastewater because of its numerous applications in manufacturing, construction, and the chemical industry.[1] Cd^{2+} contamination impairs the activity of soil enzymes,[2] interferes with water uptake, reduces photosynthesis, inhibits the root growth of plants,[3] and can lead to liver lesions, kidney diseases, osteoporosis, and various types of cancer.[4] Removing Cd from wastewater is therefore critical to meet effluent standards before it can be discharged.[5]

Various physical, chemical, and/or biological approaches have been developed to remove heavy metals from wastewater, such as photocatalysis, electrochemical treatment, ion exchange, coagulation/flocculation, nanofiltration, and adsorption.[6] Among the reported approaches, adsorption, including physical and chemical adsorption processes, has been considered as one of the easiest and most cost-effective techniques because of its strong adaptability in removing various heavy metals from aqueous solutions with simple operation.[7] Therefore, adsorption processes have been widely applied, especially in developing countries.[8] Many adsorbents have been used for Cd^{2+} adsorption, such as activated carbon, fly ash, bio-adsorbents, algae, and nanoparticles.[9–13] However, the adsorption capacity of these adsorbents is usually low, while the complex modification of adsorption materials increases the cost of the adsorbents. Therefore, the search for low-cost adsorbents with practical utility has recently attracted much attention.

Agricultural wastes have been used as a kind of low-cost biomaterial and are promising bio-adsorbents for Cd^{2+} removal because they contain many functional groups, such as carboxyl, hydroxyl, and sulfhydryl groups, which can be effectively combined with Cd^{2+}.[11] Before being used as bio-adsorbents for Cd^{2+} removal, agricultural wastes are often modified to improve their selectivity and adsorption performance. Various modification technologies for biomaterials have been explored, such as high-temperature and high-pressure treatment, material mixing, and alkali treatment,[14,15] among which, direct alkali modification is considered simpler,

[a]CAS Key Laboratory of Environmental and Applied Microbiology, Environmental Microbiology Key Laboratory of Sichuan Province, Chengdu Institute of Biology, Chinese Academy of Sciences, Chengdu 610041, China. E-mail: zhaohai@cib.ac.cn; jinyl@cib.ac.cn

[b]College of Life Science and Biotechnology, Mianyang Teachers' College, Mianyang 621000, China

[c]Crop Characteristic Resources Creation and Utilization Key Laboratory of Sichuan Province, Mianyang Academy of Agricultural Sciences, Mianyang 621023, China

safer, and more energy efficient. Hsua *et al.* reported that treating Ti–7.5Mo with NaOH resulted in better bioactive properties and exhibited a nanoscale porous network structure.[16]

Sweet potato (SP) is the sixth most abundant food crop worldwide and is rich in nutrients, including starch, crude fiber, flavonoids, and carotene.[17] The average annual yield of SP in the world from 2016 to 2020 was 91.12 million tons, and the annual production in China was approximately 51.54 million tons, accounting for 56.56% of the world's SP yield.[18] SP has a high starch content and is mostly used for starch production. However, 4.5–5.0 tons of sweet potato residue (SPR) are generated while producing 1 ton of starch,[19] which is not only a waste of resources but also harmful to the environment. SRP contains starch and other nutrients, which are easily used by microorganisms, thereafter resulting in spoilage and odor. SPR contains a large amount of useful component, that can be further used, such as lignin, cellulose, hemicellulose, protein, and pectin, which makes it suitable for wastewater treatment. For example, protein isolated from SPR was used as a frother to remove trace crystal violet dye by foaming.[20] Arachchige *et al.* showed that SPR modified with high hydrostatic pressure-assisted pectinase could effectively adsorb Pb^{2+} in wastewater.[19]

In this study, the adsorption capacity of SPR for Cd^{2+} was investigated for the first time. The SPR was modified with NaOH under optimized conditions. Then, the factors that affect the adsorption performance were evaluated. Finally, the intrinsic adsorption mechanism was elucidated by structure characterization, adsorption kinetics, and isotherms. This study demonstrates a new strategy for cost-effective Cd^{2+} removal with SPR, as well as presenting a method for the alkali modification of SPR to improve the Cd^{2+} adsorption, and revealing the mechanism of Cd^{2+} removal by the alkali-modified SPR. This provides a new idea for the utilization of SPR and the treatment of wastewater contaminated with heavy metals.

2. Materials and methods

2.1 Material preparation

The fresh SPR was collected from Jinmei Ltd (Sichuan, China), which had been separated with starch from sweet potato Xushu 22, and immediately stored at 4 °C. The cadmium chloride ($CdCl_2$, Tianjin Jinbei Fine Chemical Co., Ltd, China) was dried at 105 °C for 2 h and dissolved to the target concentration to use as simulated cadmium-containing wastewater. Sodium hydroxide (NaOH) was purchased from Chengdu Cologne Chemical Co., Ltd, China.

2.2 Experimental design

2.2.1 Optimization of the modification conditions. To improve the adsorption efficiency of the SPR, the SPR was first boiled in a water bath pot at 100 °C for 30 min, and then treated with different concentrations (0.5, 1.0, 1.5, and 2.0 M) of NaOH under different temperatures (20 °C, 30 °C, and 40 °C) for 2 h, with striation every 30 min. After treatment, the SPR was washed in multiple rounds until reaching pH 7, and then soaked with 300 mL of absolute alcohol for 24 h. After washing thoroughly to remove the remaining alcohol, the SPR was then dried in an oven (GXZ-GF101-1-BS-II, Hengzi, China) at 60 °C. Afterwards, the dried SPR was smashed by a pulverizer (JP-150A-8, Jiupin, China), and finally three different sizes (100, 150, and 300 μm) of SPR particles were chosen for the following Cd^{2+} adsorption. The modified SPR was named MSPR.

MSPR (0.3 g) was added to a 50 mL centrifuge tube containing 50 mg L^{-1} Cd^{2+} and mixed for 4 h. After adsorption, the simulated wastewater was collected and the concentration of Cd^{2+} in the water was measured by atomic adsorption spectrometry (iCE™ 3400 AAS, Thermo Scientific™, USA) to determine the optimal modification conditions for the next experiment.

2.2.2 Optimization of the adsorption conditions. The concentration of Cd^{2+} in the simulated wastewater was set to 50 mg L^{-1} at first. To adapt to the different conditions of wastewater, the pH of the simulated wastewater was adjusted to 4, 5, 6, 7, and 8 with 40% NaOH or 50% HCl, and the adsorption temperature was set to 20 °C, 30 °C, 40 °C, 50 °C, and 60 °C in an incubator (IS-RDS3, Crystal, USA). The concentrations of Cd^{2+} in the simulated wastewater were determined at 30 min intervals during a 6 h adsorption period to investigate the effect of the contact time on the adsorption process.

To investigate the effect of the adsorbent amount and Cd^{2+} initial concentrations on the removal rate, a series of MSPR amounts (0.1, 0.2, 0.3, 0.4, and 0.5 g) were added to 50 mL of simulated wastewater (Cd^{2+}, 50 mg L^{-1}), and the Cd^{2+} concentrations were set to 10, 30, 50, 70, and 90 mg L^{-1} and mixed with 0.3 g MSPR for 4 h, respectively.

2.3 Adsorption isotherms and kinetics

An equilibrium adsorption study was performed by placing 0.3 g of MSPR in 50 mL of simulated wastewater with different initial Cd^{2+} concentrations (10, 30, 50, 70, and 90 mg L^{-1}) for 4 h at 25 °C. The amount of adsorbed Cd^{2+} (q_e, mg g^{-1}) was calculated using eqn (1).

$$q_e = \frac{(C_0 - C_e)V}{W} \quad (1)$$

where C_0 and C_e represent the initial and equilibrium concentrations (mg L^{-1}), respectively, and V and W represent the volume of the solution (L) and weight of the MSPR (g), respectively. The Langmuir and Freundlich equations were used to analyze the adsorption mechanism of Cd^{2+}.

Different contact times were used to investigate the adsorption kinetics. First, 50 mL of simulated wastewater (50 mg L^{-1}, Cd^{2+}) was contacted with 0.3 g MSPR in 50 mL centrifuge tubes at 25 °C. Samples were taken at 30 min intervals to determine the changes in the Cd^{2+} concentration during a contact time of 6 h. The variation in Cd^{2+} adsorption, q_t (mg g^{-1}), was calculated using eqn (2).

$$q_t = \frac{(C_0 - C_t)V}{w} \quad (2)$$

where C_t is the concentration of Cd^{2+} (mg L^{-1}) at a given time (h), and C_0 is the initial Cd^{2+} concentration (mg L^{-1}). Pseudo-

Table 1 Adsorption model and equations

Adsorption model	Original form equation	Linearized form equation
Langmuir	$q^a = \frac{q_m^b \cdot k_L^c \cdot C^d}{1 + k_L \cdot C}$	$\frac{C}{q} = \frac{1}{k_L \cdot q_m} + \frac{1}{q_m} \cdot C$
Freundlich	$q = k_F^c \cdot C^{1/ne}$	$\log_q = \log_{k_F} + \frac{1}{n} \cdot \log C$
Pseudo-first order	$q_t^f = q_e^b(1 - e^{-kg_1 t})$	$\lg(q_e - q_t) = \lg q_e - \frac{k_1 t}{2.303}$
Pseudo-second order	$q_t = \frac{k_2^h q_e{}^2 t}{1 + k_2 q_e t}$	$\frac{t}{q_t} = \frac{1}{k_2 q_e{}^2} + \frac{t}{q_e}$

[a] q is the amount of Cd^{2+} adsorbed per specific amount of adsorbent (mg g^{-1}). [b] q_m and q_e are the saturation adsorption amount and equilibrium adsorption amount, respectively (mg g^{-1}). [c] k_L and k_F are the Langmuir and Freundlich equilibrium constants, respectively. [d] C is the equilibrium concentration of Cd^{2+} (mg L^{-1}). [e] $1/n$ is the adsorption index. [f] q_t is the amount of adsorption at time t (mg g^{-1}). [g] k_1 is the pseudo-first-order constant (min^{-1}). [h] k_2 is the pseudo-second-order constant (g (mg min^{-1})).

first-order and pseudo-second-order equations were employed to investigate the kinetic processes and mechanisms of adsorption.

The details of the Langmuir and Freundlich equations and the pseudo-first/second-order equations are shown in Table 1.[21–25]

2.4 Structural characterization

SPR, MSPR, and adsorbed MSPR (AMSPR) were collected and dried. The adsorption mechanism was further investigated by analyzing the physical and chemical properties of the three materials.

To evaluate the Brunauer–Emmet–Teller (BET)-specific surface area and pore-size distribution, the samples were degassed by vacuum to remove any impurity gas adsorbed on the surface. The degassing temperature was set to 120 °C, and the degassing time was 6 h. Then the samples were weighed and placed in liquid nitrogen, and the nitrogen adsorption capacity of the samples was determined at different pressure points set in advance to obtain the adsorption isotherm using a dedicated fully automatic specific surface and porosity analyzer BET system (Nova 4000e, Quantachrome, USA). The BET and Barrett–Joyner–Halenda (BJH) models were used to calculate the specific surface area and pore-size distribution.

Fourier-transform infrared spectroscopy (FTIR, Nicolet 6700, Thermo Scientific, USA) was used to investigate the influence of the functional groups on the adsorption process. First, 1–2 mg sample and 200 mg of KBr were mixed into a mold to form transparent flakes using an oil pressure machine. The prepared flakes were subjected to FTIR analysis and the test conditions were set at 4000–400 cm^{-1} wavelength, scanning 32 times, and resolution of 4 cm^{-1} to determine the transmittance.

To measure and analyze the surface morphology and chemical composition, SPR, MSPR, and AMSPR were analyzed as per the following methods. Since SPR is a non-conductive material, the material was sprayed with platinum (Pt) as a pretreatment for the scanning electron microscopy (SEM, Sigma 300, ZEISS, Germany) and energy dispersive X-ray (EDAX, Gemini 300, ZEISS, Germany) analysis. The samples were directly pasted to the conductive adhesive, and sprayed by a sputter coater (SC7620, Quorum, UK) with Pt for 45 s, at a current of 10 mA. Subsequently, SEM and EDAX was used to assess the sample morphology and for the energy spectrum mapping, where the accelerating voltage was 3 kV for the topography photography, 15 kV for energy spectrum mapping, using a secondary electron detector (SE2).

2.5 Data analysis

All the treatments were performed in triplicate. Microsoft Excel 16.53, IBM SPSS 22 and origin 2021 software were used to analyze the data.

3. Results and discussion

3.1 Effect of the modification conditions on Cd^{2+} removal

NaOH can de-polymerize lignin and hydrolyze hemicellulose to expose cellulose. Breaking the covalent relationship between the lignocellulose components by NaOH solution can affect the pore structure of cellulose. In addition, NaOH can also alter the chemical and mechanical properties of SPR, revealing functional groups like –OH.[26–28]

Temperature can affect the hydrolysis of starch and lignocellulose in SPR under NaOH treatment.[29] As shown in Fig. 1, the removal rate of MSPR for Cd^{2+} reached the highest values of 94.78%, 95.82%, and 95.58%, under 20 °C, 30 °C, and 40 °C, respectively, while the removal rate for the unmodified SPR was 82.67%. The highest removal rate of MSPR was obtained at 30 °C, which was 13.51% higher than that of SPR. Similar trends were also found for different NaOH concentrations and different adsorbent sizes. The effect of 30 °C modification was generally better than that of the other two temperatures, and also superior to the unmodified SPR. Therefore, 30 °C was the temperature chosen for the further adsorption experiments.

The NaOH concentration normally has a significant effect on the modification of biomaterials.[30] Under the optimal temperature of 30 °C, when using a particle size of 300 μm, 1.5 M NaOH was the best modification condition for Cd^{2+} removal, and its removal rate was 94.59% (Fig. 1(a)); whereas when particle sizes of 150 and 100 μm were used, the removal rates of SPR treated with 1.5 M and 2.0 M NaOH were quite similar with no

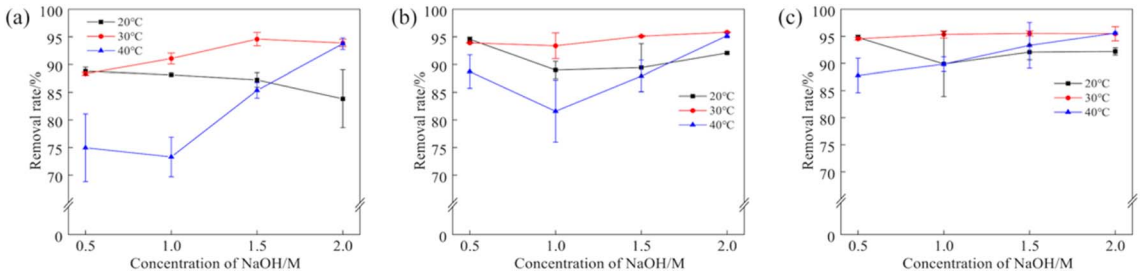

Fig. 1 The effects of temperature and NaOH concentration on the adsorption rates with (a) adsorbent size 300 μm, (b) adsorbent size 150 μm, and (c) adsorbent size 100 μm.

significant difference (p = 0.41, >0.05 and p = 0.95, >0.05), showing the higher values of 95.12% and 95.83%, and 95.52% and 95.48% respectively, than the other conditions (Fig. 1(b) and (c)). In short, at different particle sizes and 30 °C, 1.5 M and 2.0 M NaOH, especially 1.5 M NaOH, endowed SPR with better adsorption than the other conditions. Therefore, based on both the removal rate and cost considerations, 1.5 M was finally chosen as the modification concentration.

The rate of ion exchange in solution is generally controlled by the rate of ion diffusion within the adsorbent particle. A decrease in the average particle size of the adsorbent increases the surface area. Overall, the removal rate of MSPR at 300 μm particle size was lower than that of the other two particle sizes. However, the removal rates of the 100 μm and 150 μm sized particles under 1.5 M NaOH at 30 °C were similar with no significant differences (p = 0.144, >0.05). In addition, the smaller the particle size, the lower the material yield, and the higher the energy consumption for shredding. Therefore, 150 μm was chosen as the most suitable particle size.

After comprehensively consideration, SPRs modified with 1.5 M NaOH at 30 °C and a particle size of 150 μm were selected as the optimal adsorbent for the next experiments.

3.2 Characterization of the adsorbents

3.2.1 BET specific surface area and pore size. Many studies have shown that agricultural wastes have a low BET surface area, which is due to the cellulose, hemicellulose, and lignin in the lignocellulose-based biosorbents.[31] Here, SPR, MSPR, and AMSPR exhibited BET surface areas of 1.170, 0.972, and 0.883 $m^2\ g^{-1}$, respectively, which were similar to the sizes observed in other agricultural wastes, such as 0.86 $m^2\ g^{-1}$ for tea waste,[32] 0.85 $m^2\ g^{-1}$ for carnauba palm leave, 0.60 $m^2\ g^{-1}$ for macamba seed endocarp, and 0.86 $m^2\ g^{-1}$ for pine nut shells.[33] In general, a higher surface area would result in a higher ion adsorption capacity.[34,35] Interestingly, MSPR could effectively remove 95.83% of Cd^{2+}, although it had a lower BET surface area than that of SPR. It was reported that a decrease in surface area can improve heavy metal immobilization,[36] which may be one reason for the higher removal rate of MSPR than that of SPR. It was reported that modified rice husks with a low BET surface area of 1.64 $m^2\ g^{-1}$ were able to remove 95.4% of the dye methylene blue with high efficiency.[37] In addition, NaOH modification can also change the pore volume structure. In our study, the pore volume of SPR decreased after treatment with NaOH, changing from 0.0029 g cm^{-3} to 0.0023 g cm^{-3}. In a study of pitch-based activated carbon fibers, Shima *et al.* found a reduction in pore volume after modification with NaOH because the pores were blocked by newly formed functional oxide groups at the unreacted edges of the basal planes.[38] Similarly, NaOH modification might result in more functional groups formation in MSPR. After adsorption, the pore volume of MSPR was reduced to 0.0017 g cm^{-3}, for a reduction of 0.0006 g cm^{-3}, which might have resulted from the blocking of the pores by the adsorption of Cd^{2+} onto the MSPR.

The nitrogen adsorption–desorption isotherm is usually divided into six categories. It can be seen from Fig. 2(a) that the three materials were similar, with typical capillary condensation followed by hysteresis loops,[39] belonging to the IV-type isotherm. The IV-type isotherm is mainly found in mesoporous materials. There was an overlap between N_2 adsorption and desorption in Fig. 2(a). One of the reasons for this phenomenon may be that the orifices of SPR, a carbon material, shrink directly after adsorbing gas, resulting in a hard desorption of the gas from SPR, and this shrinkage together with the hard desorption can easily cause the overlap. The nitrogen adsorption–desorption isotherm indicated that SPR, MSPR, and AMSPR were mesoporous materials. Mesoporous materials are promising adsorbents because they have many pores (between 2–50 nm), and the adsorption sites are uniformly distributed on the internal and external surfaces.[40] The BJH adsorption results showed that the pore diameters in SPR, MSPR, and AMSPR were 3.475, 3.107, and 3.479 nm, respectively, all of which were in the mesoporous range. Both the pore-size determination and nitrogen adsorption–desorption isotherms showed that the MSPR is a mesoporous material that can be used as an effective adsorbent.

3.2.2 FTIR spectroscopy. Agricultural wastes, including SPR, contain a lot of functional groups, such as –OH (cellulose, lignin, and hemicellulose), –CH bonds (aliphatic and aldehyde compounds), C=C (aromatic lignin rings), –CO (carboxylic acids), and other alcohols, ethers, and phenol.[11,41] The abundant functional groups are advantageous for interactions with metal ions, such as covalent, complexation, hydrogen bonding, or other electrostatic interactions in solution.

Compared to unmodified SPR, MSPR displayed a clear peak in its FTIR spectrum at 2137 cm^{-1} (Fig. 2(b)), corresponding to

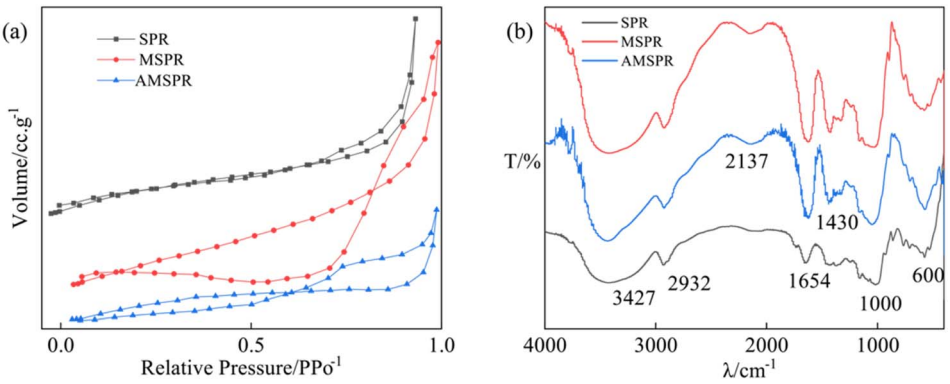

Fig. 2 (a) Nitrogen adsorption–desorption isotherms and (b) FTIR spectra of the materials.

triple bond and cumulative double bond regions, such as –C≡C, –C≡N, –C=C=C, and –C=C=O. These groups may interact with Cd^{2+} and remove Cd^{2+} from the water. Meanwhile, all three samples displayed a broad absorption peak at 3427 cm^{-1}, corresponding to the –OH groups. After modification, the peak was stronger than that of the unmodified SPR, indicating that NaOH modification might increase the amount and change the role of the functional groups. The –CH stretching of the methyl and methylene groups always occurred in the adsorbent at about 2932 cm^{-1}, which was characteristic of lignin, cellulose, and hemicellulose. The peak at 1654 cm^{-1} corresponded to the –COOH functional group, while the $–CH_2$ or O–H functional groups appeared at 1430 cm^{-1}. It was obvious that the –COOH stretching was enhanced significantly after NaOH modification. The peaks at 1000 cm^{-1} were assigned to the stretching vibrations of C–O in lignin, hemicellulose, and cellulose. Moreover, the peak at 600 cm^{-1} corresponded to the –CH of the amine group, with the mechanical vibration strength of MSPR significantly stronger than that of SPR. In the 500–800 cm^{-1} range, the functional groups of the starch or other sugars could have undergone chemical reactions.[42] The adsorbent had abundant –OH, –COOH, and –CH groups, which provide more adsorption sites.

After modification, the absorption peaks all increased to varying degrees when compared with the raw material, which could improve the interaction with Cd^{2+} and ultimately increase the removal rate. Compared with materials that were not adsorbed, the vibrational peak of the –OH group was somewhat attenuated, indicating that Cd^{2+} had reacted with the –OH group. After adsorbing Cd^{2+} from the simulated wastewater, the peak intensities of MSPR at 3427 and 2932 cm^{-1} were shifted because Cd^{2+} was exchanged with H^+ in the –OH and $–CH_2$ or $–CH_3$, and the carbonyl group could also be complexed with Cd^{2+}. In short, the change in the functional group type and content may be an important reason for the significant improvement of the MSPR adsorption ability.

3.2.3 SEM and EDAX. The morphology of the adsorbent was demonstrated using SEM. As shown in Fig. 3(a) and (b), the SPR had many round starch particles. Sweet potato is a crop rich in starch, and even after starch extraction, the SPR sample still contained a large amount of starch. Whereas MSPR did not have starch granules (Fig. 3(a) and (b)), and the removal rate of SPR was lower than that of MSPR. This may be due to the fact that starch was hydrolyzed by NaOH, which changed the morphology of the starch and produced more available functional groups.[43] The surface of the SPR was smooth and had fewer voids. After modification, the material appeared corrugated, wrinkled, and loose, forming an irregular layered shape and a microporous structure that might help create more adsorption sites for Cd^{2+} binding. This stratified structure could have been formed by cellulose, hemicellulose, and lignin. Fig. 4(c) shows the apparent morphology of AMSPR and the energy spectrum of the Cd^{2+} distribution in this region. As shown in Fig. 4(c), Cd^{2+} was uniformly distributed on the surface of AMPSR, verifying the adsorption and immobilization of Cd^{2+} in MSPR.

The EDAX spectra and elemental compositions of the materials are shown in Fig. 4. SPR, MSPR, and AMSPR were mainly composed of C and O elements and a small number of metal ions. The SPR and MSPR had no characteristic peak associated with Cd^{2+}, showing no presence of Cd^{2+} before adsorption. Whereas, the EDAX spectra showed a characteristic peak associated with Cd^{2+} (around 1.5%) for the AMSPR, confirming the presence of Cd^{2+}. After adsorption, Ca^{2+} decreased and Cd^{2+} increased on the surface of AMSPR, which could be due to the exchange of Ca^{2+} with Cd^{2+} and the simultaneous occupation by Cd^{2+} of the adsorption site of Ca^{2+}. This was also observed in a study by Liu *et al.*,[44] in which synthetic thiol-functionalized mesoporous calcium silicate was used to remove Cd^{2+}, and Ca^{2+} was exchanged with Cd^{2+}, which made a large contribution to Cd^{2+} removal. In another study, He *et al.* investigated the mechanism of adsorption of Cd^{2+} on silica–calcium phosphate hybrid nanoparticles and found that ion exchange between Cd^{2+} and Ca^{2+} in the material improved the adsorption capacity of the material.[45] Our results show that the adsorption patterns presented in the above-mentioned synthetic materials also existed in agricultural waste.

3.3 Effects of the adsorption conditions on Cd^{2+} removal

3.3.1 Effect of the initial solution pH. It has been shown in many studies that the pH of a solution is an important factor

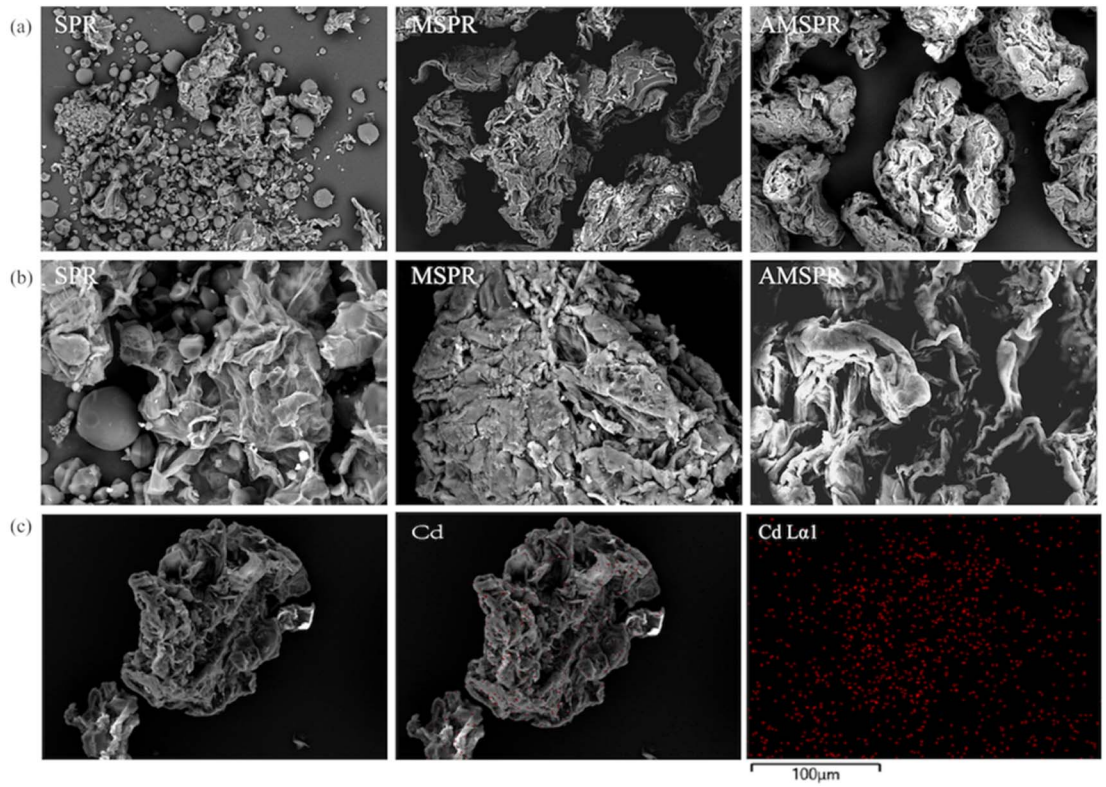

Fig. 3 SEM images of SPR under (a) 500× magnification and (b) 2000× magnification. (c) SEM images showing Cd^{2+} distribution on AMSPR. The red dots represent Cd^{2+} .

affecting the adsorption of heavy metals. This is because the pH affects not only the degree of protonation of the functional groups on the surface of the adsorbent but also the chemical properties and the forms of the heavy metal ions in the solution.[46] The adsorption efficiency of the adsorbent can change significantly when the pH is changed. As shown in Fig. 5(a), an increase in pH increased the removal rate. Between pH 4–8, the removal rate of Cd^{2+} by MSPR was above 93.00%,

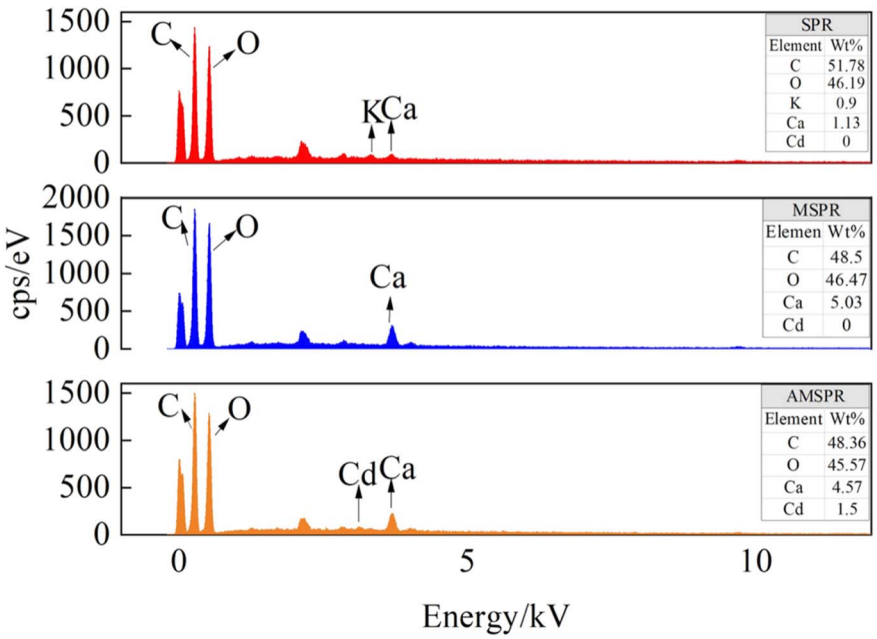

Fig. 4 EDAX spectra of the materials.

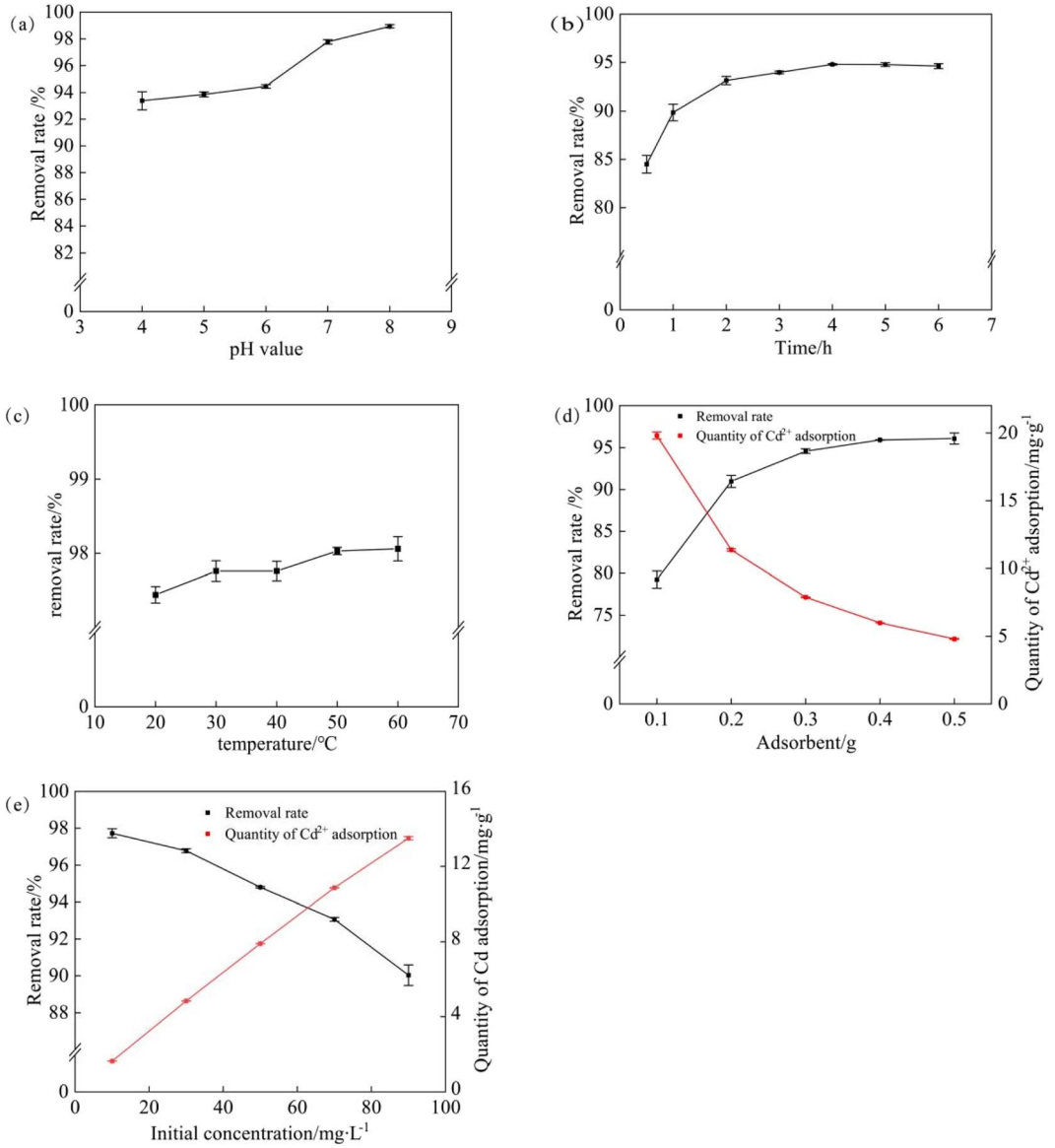

Fig. 5 Influence of the (a) pH, (b) contact time, (c) temperature, (d) adsorbent amount, and (e) initial Cd^{2+} concentration on the adsorption of Cd^{2+} by the MSPR.

and the highest removal rate of 98.94% was achieved at pH 8. The reason for this phenomenon is that the increase in pH reduces the concentration of H^+ in the solution, and the H^+ can easily combine with the oxygen-containing functional groups on the surface of MSPR and compete with Cd^{2+} for adsorption sites. Thus, increasing the pH will provide more active sites and improve the adsorption capacity of MSPR. The adsorption of Cd^{2+} in the pH range of 1–5 with tea waste was studied, and it was found that the removal rate tended to be stable (50%) at pH 4–5.[32] When adsorbing Cd^{2+} with activated carbon, the removal rates between pH 4–8 were also less than 90.00%, and presented a sharp increase.[46] In this study, Cd^{2+} adsorption by MSPR was stable and highly efficient. Therefore, it can be concluded that MSPR had a stabilizing effect on Cd^{2+} and could be adapted to different sources of heavy metal-contaminated wastewater, whose pH values are different in actual situations. Under higher pH, a hydroxide precipitate (Cd $(OH)_2$) would form, which was not within the range of our adsorption study, and thus comparisons under the higher pH value were not analyzed here.

3.3.2 Effect of the contact time. Fig. 5(b) shows the effect of the contact time on the removal rate of Cd^{2+}. The removal rate of Cd^{2+} increased with time. At 0.5 h, the removal rate reached 84.51%, indicating a rapid adsorption and removal. From 0.5 to 4 h (94.80%), the removal rate increased by 11.43%, and the adsorption capacity decreased significantly. In the initial phase of adsorption, many adsorption sites and pores are exposed on the MSPR surface. After contact with the solution, Cd^{2+} rapidly occupies these sites and fills the pores, decreasing the adsorption rate. Moreover, the removal rate did not change significantly or even decreased slightly from 4–6 h (94.62%),

indicating that desorption occurred after the adsorption equilibrium was reached at 4 h. Therefore, a contact time of 4 h was selected for the further tests.

3.3.3 Effect of temperature. The temperature of wastewater varies depending on the sources and seasons. Generally, temperature affects the thermal motion of molecules, the diffusion rate of the adsorbate in the adsorbent pores, and the adsorption rate.[47] High temperatures can easily lead to a desorption of the adsorbate, while low temperatures affect the diffusion rate and adsorption rate of the adsorbate in the pores. Fig. 5(c) shows the relationship between the adsorption temperature and the removal rate. The results indicated that the removal rate was only slightly improved at temperatures from 20 °C to 60 °C, with an overall stability of approximately 97.00%. At 60 °C, the removal rate of Cd^{2+} by MSPR reached 98.06%, with an improvement of 15.39% compared with SPR. In the study of Cd^{2+} adsorption by a chitosan–silica hybrid aerogel, the removal rate of Cd^{2+} showed a downward trend with the increase in adsorption temperature.[48] In another study of Cd^{2+} removal from duckweed, the adsorption temperature was set at 15–45 °C, and the Cd^{2+} removal rate was less than 70%.[42] However, the removal rate of Cd^{2+} varied slowly by MSPR, from 97.44% to 98.06% when the temperature was increased from 20 °C to 60 °C, indicating that temperature had little effect on the adsorption performance of MSPR. Therefore, MSPR may be used in wastewater treatment in a wide temperature range.

3.3.4 Effect of the adsorbent amount. The amount of adsorbent is also one of important factors that affect the adsorption. Fig. 5(d) shows that the removal rate increased with the increase in adsorbent amount, and this was observed with greater intensity when 0.1 and 0.2 g were used, going from 79.24% to 90.98%, respectively, and then stabilizing at about 95.00% at 0.3–05 g. The opposite trend was observed in the adsorption capacity, which decreased with the increasing amount of adsorbent, from 19.81 to 4.81 mg g^{-1}. The highest adsorption capacity of MSPR (19.81 mg g^{-1}) was 3.32 times that of SPR (5.97 mg g^{-1}), which was comparable to the value of around 1.5% determined by spectroscopic scanning. The adsorption capacity of MSRP (19.81 mg g^{-1}) for Cd^{2+} was higher than that of many other agricultural wastes, such as okra waste (14.80 mg g^{-1}),[49] cinnamon woodchips biochar (5.31 mg g^{-1}),[50] green longan hull (4.19 mg g^{-1}), and brewed tea waste (2.47 mg g^{-1}),[51,52] which to some extent showed its advantages over many other agricultural wastes for Cd^{2+} adsorption. From 0.3–0.5 g, the removal rate stabilized. A higher adsorbent amount provided more adsorption sites and pore volume and increased the probability of interaction with Cd^{2+} providing the number of Cd^{2+} ions was greater than the number of adsorption sites. When the required adsorption sites for Cd^{2+} were much smaller than that provided by the MSPR, the probability of binding Cd^{2+} to the adsorption site on the MSPR was relatively low, although the removal rate increased, and the final adsorption capacity was reduced. Therefore, 0.3 g was determined as the best suitable amount for the dosage for the further research.

3.3.5 Effect of the initial Cd^{2+} concentration. The effects of different initial Cd^{2+} concentrations on the removal efficiency are shown in Fig. 5(e), including effects on the adsorption capacity and removal rate. A linear upward trend and a 1.26-fold improvement in the final adsorption capacity of 13.51 mg g^{-1} compared with SPR were observed when the initial Cd^{2+} concentration was 90 mg L^{-1}. This may be attributed to the fact that at lower Cd^{2+} concentrations, there is a larger amount of available adsorption sites for few Cd^{2+}, resulting in a lower adsorption capacity. However, with increasing the Cd^{2+} concentration, the ions occupied the entire adsorption sites and the final adsorption capacity increased. However, with increasing the Cd^{2+} concentration, the removal rate showed a downward trend, and Cd^{2+} may remain in the solution because of the limited number of active sites on the adsorbent. In spite of this, the removal rates of MSPR were higher than 90% when the Cd^{2+} concentrations were 10–90 mg L^{-1}. Similarly, with the increase in the initial Cd^{2+}concentration, a downward trend in the removal rate was also found in terms of the Cd^{2+} adsorption with an activated carbon/zirconium oxide composite, while the removal rate was lower than 80%,[14] which was definitely lower than that of MSPR. This indicated that MSPR could better adapt to different concentrations of Cd^{2+}-containing effluents.

In short, the removal rates of MSPR under different pH, temperature, and initial concentration of treatment conditions were always more than 90%. Besides, the removal of Cd^{2+} by MSPR was a fast process, and 90% of the Cd^{2+} in water could be removed with 1 h.

3.4 Adsorption isotherms and kinetics

3.4.1 Isotherms. Adsorption is divided into chemical and physical adsorption, depending on the strength of the interaction between the adsorbate and the adsorbent. Weak electrostatic interactions are classified as physical adsorption, while chemical bond formation is classified as chemical adsorption. In chemical adsorption, a single layer of the adsorbate forms on the adsorbent, whereas in physical adsorption, multiple layers of adsorbate form. The representatives of the two models are the Langmuir and Freundlich models. Both are empirical equations.

Fig. 6(a) and Table 2 show the fitting results of the Langmuir and Freundlich models, respectively.

As shown in Table 2, the R^2 of the Langmuir isotherm (0.9914) was larger than that of the Freundlich isotherm (0.9847), which was a better fit for this adsorption curve. The Langmuir adsorption equation is defined as a single-layer adsorption isotherm in which the chemisorption and adsorption vacancies reach equilibrium on a surface with a uniform energy distribution. This fitting results showed that the adsorption process of Cd^{2+} by MSPR was single-layer surface adsorption; all the adsorption sites were the same, and there was no interaction between the Cd^{2+} ions, which was a characteristic of chemical adsorption. Also, k_L is the equilibrium constant of adsorption, and a larger value represents a stronger adsorption capacity. In a study on the removal of Cd^{2+} from contaminated wastewater with poplar sawdust, the highest k_L was 0.017.[53] In another study, the k_L of an activated carbon/zirconium oxide composite was 0.059.[47] The k_L obtained in this study was 0.348, which was greater than that of the

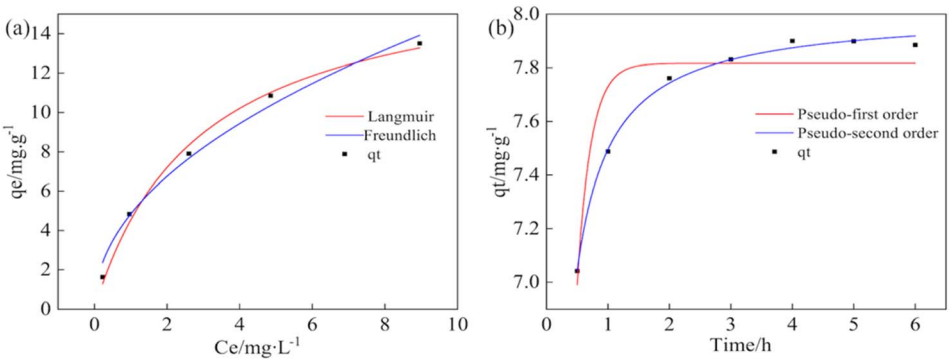

Fig. 6 (a) Langmuir and Freundlich equilibrium isotherm modeling for Cd^{2+} adsorption by MSPR and (b) pseudo-first/second-order kinetic plot of the MSPR.

Table 2 Langmuir, Freundlich, pseudo-first-order, and pseudo-second-order parameters for the adsorption of Cd^{2+} onto MSPR

Model	Parameter	Modified sweet potato residue
Langmuir	q_m (mg g^{-1})	17.53
	k_L (mg L^{-1})	0.35
	R^2	0.9914
Freundlich	n	2.07
	k_F	4.83
	R^2	0.9847
Pseudo-first order	q_m (mg g^{-1})	7.82
	k_1 (mg L^{-1})	44 945
	R^2	0.8382
Pseudo-second order	q_m	8.01
	k_2	7393.47
	R^2	0.9957

common materials used to adsorb Cd^{2+}, indicating that the potential ability of MSPR to adsorb Cd^{2+} was stronger.

3.4.2 Kinetics. There are several models for adsorption kinetics, such as the pseudo-first order, pseudo-second order, mixed order, and Ritchie's equations. The pseudo-first-order and pseudo-second-order models, which also are empirical models, are the most commonly used in the study of the adsorptive removal of pollutants from an aqueous phase.

The pseudo-first-order and pseudo-second-order fitting results are shown in Fig. 6(b) and Table 2. In terms of the curve fitting and R^2, the kinetics of Cd^{2+} adsorption by MSPR was better fitted with the pseudo-second-order model (R^2 values of 0.996) than the pseudo-first-order model (R^2 values of 0.838) (Table 2). The pseudo-second-order rate expression is used to describe chemisorption involving valency forces through the sharing or exchange of electrons between the adsorbent and the adsorbate as covalent forces and ion exchange, which are assumed to occur *via* chemisorption. In the study of the adsorption of Cd^{2+} by iron/manganese binary metal oxide-biochar nanocomposites, the R^2 of the pseudo-second-order fitting equation was found to be greater than the first, which indicated it belonged to chemical adsorption, less than physical adsorption.[54] The higher R^2 of the pseudo-second-order model indicated that MSPR in contact with Cd^{2+} is a chemical adsorption process, and the adsorption rate is determined by the concentration of Cd^{2+} and the amount of adsorbent.

Based on the results of both the adsorption isotherms and kinetics, we could deduce that the adsorption of Cd^{2+} by MSPR was a process dominated by chemical adsorption.

4. Conclusion

Our research suggested a possibility of using MSPR as an economical adsorbent for Cd^{2+} removal from wastewater. The optimum modification conditions were determined as follows: a concentration of 1.5 M NaOH, a reaction temperature of 30 °C, and a particle size of 150 μm. The removal rate of Cd^{2+} increased with the contact time and the amount of adsorbent added. MSPR could adapt well to a wide pH range and adsorption temperatures, with a highest removal rate of 98.94% and an adsorption capacity of up to 19.81 mg g^{-1}. The MSPR had rich functional groups, a loose surface, and a mesoporous structure, as determined by BET, FTIR, and SEM analyses. The EDAX results showed that AMSPR exhibited distinct Cd^{2+}-related peaks. The adsorption kinetics and isotherms analyses showed good agreement with the Langmuir model and pseudo-second-order model, indicating that the process of adsorption of Cd^{2+} by MSPR could be characterized by chemical adsorption in single molecular layers. This study demonstrates that MSPR can effectively adsorb Cd^{2+}. Using MSPR, an abundant agricultural waste, to remove Cd^{2+} from wastewater is beneficial to reduce the cost of wastewater treatment and relieve environmental pollution brought about by waste discharge from sweet potato processing.

Data availability

Data can be required to the corresponding author.

Author contributions

Yu Gao: writing—original draft, processing data, and analysis. Zhuolin Yi: writing—review and editing. Jinling Wang: validation, software. Fan Ding: conceptualization. Yang Fang: project administration. Anping Du: investigation. Yijia Jiang: methodology. Hai Zhao: funding acquisition. Yanling Jin: upervision,

visualization, methodology, writing—review. All authors have read and agreed to the published version of the manuscript.

Conflicts of interest

There are no conflicts of interest to declare.

Acknowledgements

This work was financially supported by the earmarked fund for CARS-10-Sweetpotato (CARS-10-GW24), the Sichuan Science and Technology Program (2022YFN0043), and CAS "Light of West China" Program (2020XBZG_XBQNXZ_A_001).

References

1 Q. Li, G. Liu, L. Qi, H. Wang, Z. Ye and Q. Zhao, Heavy metal-contained wastewater in China: Discharge, management and treatment, *Sci. Total Environ.*, 2022, **808**, 152091, DOI: 10.1016/j.scitotenv.2021.152091.

2 J. Liu, Y. Li, D. Li, Y. Wang and S. Wei, The burden of coronary heart disease and stroke attributable to dietary cadmium exposure in Chinese adults, 2017, *Sci. Total Environ.*, 2022, **825**, 153997, DOI: 10.1016/j.wri.2014.07.003.

3 M. T. Hayat, M. Nauman, N. Nazir, S. Ali and N. Bangash, *Cadmium Toxicity and Tolerance in Plants*, 2019, pp. 163–183.

4 G. Genchi, M. S. Sinicropi, G. Lauria, A. Carocci and A. Catalano, The Effects of Cadmium Toxicity, *Int. J. Environ. Res. Public Health*, 2020, **17**, 3782, DOI: 10.3390/ijerph17113782.

5 M. Kumar, A. Kushwaha, L. Goswami, A. K. Singh and M. Sikandar, A review on advances and mechanism for the phycoremediation of cadmium contaminated wastewater, *Clean. Eng. Technol.*, 2021, **5**, 100288, DOI: 10.1016/j.clet.2021.100288.

6 T. A. Saleh, M. Mustaqeem and M. Khaled, Water treatment technologies in removing heavy metal ions from wastewater: A review, *Environ. Nanotechnol., Monit. Manage.*, 2022, **17**, 100617, DOI: 10.1016/j.enmm.2021.100617.

7 S. Rajendran, A. K. Priya, P. S. Kumar, T. K. A. Hoang, K. Sekar, K. Y. Chong, K. S. Khoo, H. S. Ng and P. L. Show, A critical and recent developments on adsorption technique for removal of heavy metals from wastewater-A review, *Chemosphere*, 2022, **303**, 135146, DOI: 10.1016/j.chemosphere.2022.135146.

8 Y. Zhan, Z. Ye, L. Wang, L. Yang and Y. Li, Removal of Cd (II) by polystyrene-base chelating resins: adsorption properties and experiences of industrial wastewater treatment, *Desalin. Water Treat.*, 2013, **52**(34–36), 6481–6491, DOI: 10.1080/19443994.2013.821032.

9 R. Leyva-Ramos, J. R. Rangel-Mendez, J. Mendoza-Barron, L. Fuentes-Rubio and R. M. Guerrero-Coronado, Adsorption of cadmium(II) from aqueous solution onto activated carbon, *Water Sci. Technol.*, 1997, **35**(7), 205–211, DOI: 10.1016/S0273-1223(97)00132-7.

10 B. Gabriela, L. Nicoleta, C. Horia, C. Gabriela, B. Roxana-Dana, B. Daniel, F. Lidia and H. Maria, Performance assessment of five adsorbents based on fly ash for removal of cadmium ions, *J. Mol. Liq.*, 2021, **333**(333), 115932, DOI: 10.1016/j.molliq.2021.115932.

11 M. M. Kwikima, S. Mateso and Y. Chebude, Potentials of agricultural wastes as the ultimate alternative adsorbent for cadmium removal from wastewater. A review, *Sci. Afr.*, 2021, **13**, e00934, DOI: 10.1016/j.sciaf.2021.e00934.

12 V. Jayakumar, S. Govindaradjane, P. Senthil Kumar, N. Rajamohan and M. Rajasimman, Sustainable removal of cadmium from contaminated water using green alga - Optimization, characterization and modeling studies, *Environ. Res.*, 2021, **199**, 111364, DOI: 10.1016/j.envres.2021.111364.

13 K. Hachem, D. Bokov, M. D. Farahani, B. Mehdizade and A. A. Kazemzadeh Farizhandi, Ultrasound-assisted adsorption of dyes and cadmium ion from aqueous solutions by ZnAl2O4 nanoparticles, *Mater. Chem. Phys.*, 2022, **276**, 125398, DOI: 10.1016/j.matchemphys.2021.125398.

14 G. Sharma and M. Naushad, Adsorptive removal of noxious cadmium ions from aqueous medium using activated carbon/zirconium oxide composite: Isotherm and kinetic modelling, *J. Mol. Liq.*, 2020, **310**, 113025, DOI: 10.1016/j.molliq.2020.113025.

15 R. F. Susanti, R. G. R. Wiratmadja, H. Kristianto, A. A. Arie and A. Nugroho, Synthesis of high surface area activated carbon derived from cocoa pods husk by hydrothermal carbonization and chemical activation using zinc chloride as activating agent, *Mater. Today: Proc.*, 2022, **63**, S55–S60, DOI: 10.1016/j.matpr.2022.01.042.

16 H. C. Hsua, S. K. Hsu, S. C. Wu, Y. H. Hung and W. F. Ho, Surface modification of nanotubular anodized Ti–7.5Mo alloy using NaOH treatment for biomedical application, *Thin Solid Films*, 2020, **710**, 138273, DOI: 10.1016/j.tsf.2020.138273.

17 M. K. Alam, A comprehensive review of sweet potato (*Ipomoea batatas* [L.] Lam): Revisiting the associated health benefits, *Trends Food Sci. Technol.*, 2021, **115**, 512–529, DOI: 10.1016/j.tifs.2021.07.001.

18 FAO, *Food and Agriculture Organization of the United Nations*, 2021, (Accessed 2016 2022).

19 M. P. M. Arachchige, T. Mu and M. Ma, Effect of high hydrostatic pressure-assisted pectinase modification on the Pb^{2+} adsorption capacity of pectin isolated from sweet potato residue, *Chemosphere*, 2021, **262**, 128102, DOI: 10.1016/j.chemosphere.2020.128102.

20 N. Hu, K. Zhang, Y. Zhao, Z. Zhang and H. Li, Flotation-based dye removal system: Sweet potato protein fabricated from agro-industrial waste as a collector and frother, *J. Cleaner Prod.*, 2020, **269**, 122121, DOI: 10.1016/j.jclepro.2020.122121.

21 M. S. iban, B. Radetic, Z. Kevrešan and M. Klašnja, Adsorption of heavy metals from electroplating wastewater by wood sawdust, *Bioresour. Technol.*, 2007, **98**(2), 402–409, DOI: 10.1016/j.biortech.2005.12.014.

22 K. L. Tan and B. H. Hameed, Insight into the adsorption kinetics models for the removal of contaminants from

aqueous solutions, *J. Taiwan Inst. Chem. Eng.*, 2017, **74**, 25–48, DOI: 10.1016/j.jtice.2017.01.024.

23 M. A. Al-Ghouti and D. A. Da'ana, Guidelines for the use and interpretation of adsorption isotherm models: A review, *J. Hazard. Mater.*, 2020, **393**, 122383, DOI: 10.1016/j.jhazmat.2020.122383.

24 J. Wang and X. Guo, Adsorption kinetic models: Physical meanings, applications, and solving methods, *J. Hazard. Mater.*, 2020, **390**, 122156, DOI: 10.1016/j.jhazmat.2020.122156.

25 P. Su, X. Gao, J. Zhang, R. Djellabi, B. Yang, Q. Wu and Z. Wen, Enhancing the adsorption function of biochar by mechanochemical graphitization for organic pollutant removal, *Front. Environ. Sci. Eng.*, 2021, **15**(6), 130, DOI: 10.1007/s11783-021-1418-2.

26 S. N. Jain and P. R. Gogate, NaOH-treated dead leaves of Ficus racemosa as an efficient biosorbent for Acid Blue 25 removal, *Int. J. Environ. Sci. Technol.*, 2016, **14**(3), 531–542, DOI: 10.1007/s13762-016-1160-7.

27 S. D. Ashrafi, H. Kamani and A. H. Mahvi, The optimization study of direct red 81 and methylene blue adsorption on NaOH-modified rice husk, *Desalin. Water Treat.*, 2014, **57**(2), 738–746, DOI: 10.1080/19443994.2014.979329.

28 S. Chakraborty, S. Chowdhury and P. Das Saha, Adsorption of Crystal Violet from aqueous solution onto NaOH-modified rice husk, *Carbohydr. Polym.*, 2011, **86**(4), 1533–1541, DOI: 10.1016/j.carbpol.2011.06.058.

29 B. Tatiana and N. Patrick, Cellulose in NaOH–water based solvents: a review, *Cellulose*, 2015, **23**(1), 5–55, DOI: 10.1007/s10570-015-0779-8.

30 C. Wang, J. Yu, K. Feng, H. Guo and L. Wang, Alkali treatment to transform natural clinoptilolite into zeolite Na-P: Influence of NaOH concentration, *J. Phys. Chem. Solids*, 2022, **168**, 110827, DOI: 10.1016/j.jpcs.2022.110827.

31 Y. L. d O. Salomón, J. Georgin, D. S. P. Franco, M. S. Netto, P. Grassi, D. G. A. Piccilli, M. L. S. Oliveira and G. L. Dotto, Powdered biosorbent from pecan pericarp (Carya illinoensis) as an efficient material to uptake methyl violet 2B from effluents in batch and column operations, *Adv. Powder Technol.*, 2020, **31**(7), 2843–2852, DOI: 10.1016/j.apt.2020.05.004.

32 S. Wan, Z. Ma, Y. Xue, M. Ma, S. Xu, L. Qian and Q. Zhang, Sorption of Lead(II), Cadmium(II), and Copper(II) Ions from Aqueous Solutions Using Tea Waste, *Ind. Eng. Chem. Res.*, 2014, **53**(9), 3629–3635, DOI: 10.1021/ie402510s.

33 V. d S. Lacerda, J. B. L. p. Sotelo, A. C. Guimaraes, S. H. n. Navarro, M. S. n B. scones, L. M. N. Gracia, P. M. n. Ramos and J. s M. n. Gil, Rhodamine B removal with activated carbons obtained from lignocellulosic waste, *J. Environ. Manage.*, 2015, **155**, 67–76, DOI: 10.1016/j.jenvman.2015.03.007.

34 R. Shwetharani, A. Poojashree, G. R. Balakrishna and M. S. Jyothi, La activated high surface area titania float for the adsorption of Pb(ii) from aqueous media, *New J. Chem.*, 2018, **42**(2), 1067–1077, DOI: 10.1039/C7NJ03358C.

35 M. Abdouss, A. M. Shoushtari, A. M. Simakani, S. Akbari and A. Haji, *Citric Acid-Modified Acrylic Micro and Nanofibers for Removal of Heavy Metal Ions from Aqueous Media*, 11th World Filtration Congress, 2012.

36 L. Mao, Y. Wu, W. Zhang and Q. Huang, The reuse of waste glass for enhancement of heavy metals immobilization during the introduction of galvanized sludge in brick manufacturing, *J. Environ. Manage.*, 2019, **231**, 780–787, DOI: 10.1016/j.jenvman.2018.10.120.

37 J. Ponce, J. o G. d S. Andrade, L. N. d. Santos, M. K. Bulla, B. C. B. Barros, N. H. Silvia Luciana Favaroc, W. Caetano and V. R. Batistela, Alkali pretreated sugarcane bagasse, rice husk and corn husk wastes as lignocellulosic biosorbents for dyes, *Carbohydr. Polym. Technol. Appl.*, 2021, **2**, 100061, DOI: 10.1016/j.carpta.2021.100061.

38 J. W. Shima, S. J. Parkb and S. K. Ryu, Effect of modification with HNO3 and NaOH on metal adsorption by pitch-based activated carbon fibers, *Carbon*, 2001, **39**(11), 1635–1642, DOI: 10.1016/S0008-6223(00)00290-6.

39 H. Zhang, H. Zhao, S. Mu, J. Cai, Y. Xiang, J. Wang and J. Hong, Surface relaxation and permeability of cement pastes with hydrophobic agent: Combining 1H NMR and BET, *Constr. Build. Mater.*, 2021, **311**, 125264, DOI: 10.1016/j.conbuildmat.2021.125264.

40 Y. He, Y. Hao, J. Shen, C. Wang and Y. Wei, Removal of adsorption sites on the external surface of mesoporous adsorbent for eliminating the interference of proteins in enrichment of phosphopeptides/nucleotides, *Anal. Chim. Acta*, 2021, **1178**, 338849, DOI: 10.1016/j.aca.2021.338849.

41 A. V. r. Filho,L. V. Tholozan, E. O. d. Silva, L. Meili, A. R. F. d. Almeida and G. S. d Rosa, *Biomass-Derived Materials for Environmental Applications*, 2022, pp. 243–266.

42 C. LanChai, F. Yang, J. Y. Ling, C. Qian, Z. Y. Gui, X. Yao and Z. Hai, Biosorption of $Cd^{2+}$by untreated dried powder of duckweedLemna aequinoctialis, *Desalin. Water Treat.*, 2013, **53**(1), 183–194, DOI: 10.1080/19443994.2013.839399.

43 A. Akinterinwa, E. Oladele, A. Adebayo, O. Ajayi, O. O. Iyanu and E. Gurgur, Cross-linked-substituted (esterified/etherified) starch derivatives as aqueous heavy metal ion adsorbent: a review, *Water Sci. Technol.*, 2020, **82**(1), 1–26. https://iwaponline.com/wst/article-pdf/doi/10.2166/wst.2020.332/713230/wst2020332.

44 L. Liu, T. Li, G. Yang, Y. Wang, A. Tang and Y. Ling, Synthesis of thiol-functionalized mesoporous calcium silicate and its adsorption characteristics for heavy metal ions, *J. Environ. Chem. Eng.*, 2017, **5**(6), 6201–6215, DOI: 10.1016/j.jece.2017.11.046.

45 Y. He, L. Luo, S. Liang, M. Long and H. Xu, Synthesis of mesoporous silica-calcium phosphate hybrid nanoparticles and their potential as efficient adsorbent for cadmium ions removal from aqueous solution, *J. Colloid Interface Sci.*, 2018, **525**, 126–135, DOI: 10.1016/j.jcis.2018.04.037.

46 M. Kavand, P. Eslami and L. Razeh, The adsorption of cadmium and lead ions from the synthesis wastewater with the activated carbon: Optimization of the single and binary systems, *J. Water Process. Eng.*, 2020, **34**, 101151, DOI: 10.1016/j.jwpe.2020.101151.

47 A. Akisawa, A. Tamogami, N. Takeda, M. Nakayama and T. Natsui, Effect of Adsorbent on the Performance of

Double Effect Adsorption Refrigeration Cycle with Adsorption Heat Recovery, *Int. J. Refrig.*, 2022, **141**, 21–30, DOI: **10.1016/j.ijrefrig.2022.06.012**.

48 E. Kelechi, E. O. Afamefuna, K. A. Kenneth and J. A. Ojo, Thermodynamic study of the adsorption of Cd^{2+} and Ni^{2+} onto chitosan – Silica hybrid aerogel from aqueous solution, *Results Chem.*, 2023, **5**, 100730, DOI: **10.1016/j.rechem.2022.100730**.

49 B. Y. Z. Hiew, L. Y. Lee, X. J. Lee, S. Thangalazhy-Gopakumar and S. Gan, Utilisation of environmentally friendly okara-based biosorbent for cadmium(II) removal, *Environ. Sci. Pollut. Res.*, 2020, **28**(30), 40608–40622, DOI: **10.1007/s11356-020-09594-3**.

50 X. Li, Y. Huang, X. Liang, L. Huang, L. Wei, X. Zheng, H. A. Albert, Q. Huang, Z. Liu and Z. Li, Characterization of biochars from woody agricultural wastes and sorption behavior comparison of cadmium and atrazine, *Biochar*, 2022, **4**(1), 27, DOI: **10.1007/s42773-022-00132-7**.

51 X. Guo, S. Tang, Y. Song and J. Nan, Adsorptive removal of Ni^{2+} and Cd^{2+} from wastewater using a green longan hull adsorbent, *Adsorpt. Sci. Technol.*, 2017, **36**(1–2), 762–773, DOI: **10.1177/0263617417722254**.

52 H. Çelebi, G. Gök and O. Gök, Adsorption capability of brewed tea waste in waters containing toxic lead(II), cadmium (II), nickel (II), and zinc(II) heavy metal ions, *Sci. Rep.*, 2020, **10**(1), 17570, DOI: **10.1038/s41598-020-74553-4**.

53 S. Cheng, Y. Liu, B. Xing, X. Qin, C. Zhang and H. Xia, Lead and cadmium clean removal from wastewater by sustainable biochar derived from poplar saw dust, *J. Cleaner Prod.*, 2021, **314**, 128074, DOI: **10.1016/j.jclepro.2021.128074**.

54 J. Qu, N. Che, G. Niu, L. Liu, C. Li and Y. Liu, Iron/manganese binary metal oxide-biochar nano-composites with high adsorption capacities of Cd^{2+}: Preparation and adsorption mechanisms, *J. Water Process. Eng.*, 2023, **51**, 103332, DOI: **10.1016/j.jwpe.2022.103332**.